



The Influence of Time, Tide, and Place on Fine-Scale Nekton Distribution: Insights from the San Francisco Estuary

Matthew J. Young¹ · Frederick Feyrer¹ · Jason Hassrick² · Shawn Acuña⁴ · David Ayers³ · John Donovan¹ · Lenny Grimaldo⁵

Received: 26 April 2023 / Revised: 11 March 2024 / Accepted: 14 March 2024 / Published online: 18 April 2024
This is a U.S. Government work and not under copyright protection in the US; foreign copyright protection may apply 2024

Abstract

The location of estuarine organisms varies based on geophysical cycles and environmental conditions, which can strongly bias understanding of organism abundance and distribution. In the San Francisco Estuary, California, extensive monitoring surveys have provided insight into the life history and ecology of certain commercially important or legislatively protected fish species. However, there remains substantial uncertainty in factors influencing the vertical and lateral distributions of many other nekton species in the San Francisco Estuary, including longfin smelt *Spirinchus thaleichthys*, for whom such distributional information may highly influence interpretation of existing data. We carried out paired sampling using surface and demersal gears to address three questions: (1) Does diel phase influence the vertical position of nekton (e.g., surface versus demersal)? (2) Do environmental conditions, specifically turbidity, influence the vertical and lateral positions of nekton (e.g., center channel versus peripheral shoal)? (3) Does tidal variability influence vertical and lateral distributions of nekton? We documented variability in sampled nekton densities across diel phase (day/night), vertical position (surface/bottom), and lateral position (channel/shoal). Tidal phase and turbidity concentration influenced vertical and lateral distributions for some species at certain locations. Although infrequently encountered, we documented associations of longfin smelt with the lower water column and shoal habitats, with some evidence for upward vertical shifts in low light conditions brought about by nightfall or elevated turbidity. Observed habitat associations provide insight into how interacting geophysical and environmental factors may influence the distribution of nekton and thus the vulnerability of individual species to detection by sampling gears.

Keywords Hydrodynamics · Microhabitat · Fish · Tidal stream transport · Geophysical cycles

Introduction

Estuarine species are found at the intersection of physiologically acceptable salinity levels and appropriate structural and hydrodynamic habitat characteristics (Peterson 2003).

Species-habitat relationships are especially challenging to study in estuarine ecosystems because tidal and freshwater flows create dynamic interactions with static habitat features (Cloern and Jassby 2012). Our understanding of species-habitat relationships is further complicated by various biological needs (e.g., foraging or refuge (Rountree and Able 2007) and ontogenetic development (Amorim et al. 2018)) that can necessitate movements across habitat boundaries. For example, reduced predation risk or higher food availability can drive vertical distribution within the water column, typically associated with diel cycles and low light periods (Neilson and Perry 1990; Power 1997; Mehner 2012). Organisms may also adjust their vertical position within the water column to leverage tidal hydrodynamics for directional transport and retention to and within favorable regions (selective tidal stream transport; Forward and Tankersley 2001). Lateral movements to shallow-water habitats (e.g., shoals) can offer similar low-velocity habitat for transport or

Communicated by James Allen Nelson

✉ Matthew J. Young
mjyoung@usgs.gov

¹ California Water Science Center, U.S. Geological Survey, Sacramento, CA 95819, USA

² ICF, Jones and Stokes, Inc, 980 9th Street, Suite 1200, Sacramento, CA 95819, USA

³ University of California, Davis, Davis, USA

⁴ Metropolitan Water District, Los Angeles, CA, USA

⁵ California Department of Water Resources, Sacramento, CA, USA

retention and refuge (Feyrer et al. 2013; Bennett and Burau 2015). Due to this variability in vertical or lateral position, measurements taken at certain tides or times of day can bias our understanding of abundance and distribution (Dornburg et al. 2017).

In the San Francisco Estuary, California, there is an extensive network of fisheries-independent monitoring surveys designed to understand the impacts of California's complex water management on the estuarine fish community (Stompe et al. 2020; Tempel et al. 2021). These surveys have provided insight into the life history and ecology of recreationally valuable and legislatively protected fish species, documenting distribution shifts and abundance declines for many estuarine species (e.g., Sommer et al. 2007, 2011; Mac Nally et al. 2010; Thomson et al. 2010). However, efforts to understand the effects of diel phase, tide, and water quality conditions on the vertical and lateral distributions of estuarine organisms has largely focused on planktonic organisms or planktonic life stages (Kimmerer et al. 1998; Bennett et al. 2002), recreationally important striped bass *Morone saxatilis* (Sommer et al. 2011), and state and federally endangered delta smelt *Hypomesus transpacificus* (Feyrer et al. 2013; Bennett and Burau 2015). Results from these studies provide context for understanding spatiotemporal distribution patterns in each study organism. For example, delta smelt frequently change vertical and lateral positions with changes in tidal current magnitude and direction to facilitate retention or upstream movement, exhibiting behavioral responses that appear to vary with local physical and biological conditions (Feyrer et al. 2013) and impact interpretation of various fishery-independent surveys (Bever et al. 2016). These findings help contextualize delta smelt distributional data with respect to season, life history stage, and tidal environment; however, similar insights into other at-risk or declining species in the San Francisco Estuary are limited.

One such declining species in the San Francisco Estuary is the longfin smelt *Spirinchus thaleichthys*, an anadromous fish in the family Osmeridae with annual abundance indices that have declined to historical lows in recent decades (Sommer et al. 2007; Hobbs et al. 2017), resulting in its current status as a threatened species under the California Endangered Species Act (California Fish and Game Commission 2009). Many studies have documented single-factor habitat associations for longfin smelt in the San Francisco Estuary and elsewhere. For example, surface and demersal gears catch juvenile and adult longfin smelt in the San Francisco Estuary that tend to be more associated with deeper channels rather than lateral shoals (Rosenfield and Baxter 2007), while larval longfin smelt distribution varies within the water column (Bennett et al. 2002) and across turbidity levels (Mahardja et al. 2017). Elsewhere, in Lake Washington, Washington, USA, longfin smelt exhibit strong vertical migrations associated with day/night cycles (Chigbu et al. 1998).

The effects of these elements (e.g., vertical and lateral habitats, turbidity, and diel phase) on many San Francisco Estuary nekton have not been assessed, even though variability in vertical or lateral distribution by individuals may influence interpretation of existing data. These interpretations are relevant to longfin smelt and other fish species that have declined in population (striped bass, threadfin shad *Dorosoma petenense*, Sommer et al. 2007) or shifted distribution within the San Francisco Estuary (northern anchovy *Engraulis mordax*, Kimmerer 2006), and other nekton for which limited distributional data are available (e.g., native and non-native shrimps of the infraorder Caridea). Identifying fine-scale distributional drivers for these and other species with differing behaviors and life histories can provide context for fisheries-independent monitoring programs that sample irrespective of vertical position (e.g., only surface or demersal gears), lateral position (e.g., only in channels), or tide phase.

The goal of our study was to determine if geophysical (e.g., diel and tidal cycles) and environmental conditions influence the vertical and lateral distributions of longfin smelt and other fishes and invertebrates (i.e., nekton) in the upper San Francisco Estuary. We conducted a phased program of multiple field investigations across consecutive years to address three questions related to longfin smelt and other nekton: (1) Do diel phase and other factors influence vertical position (e.g., surface versus demersal)? (2) Do environmental conditions, specifically turbidity, influence vertical and lateral positions (e.g., center channel versus peripheral shoal)? (3) Does a more nuanced assessment of tidal variability influence understanding of vertical and lateral distributions? This study provides insight into the effect of environmental conditions on the distribution of nekton within the San Francisco Estuary, and into factors that can influence the vulnerability of individual species to detection by specific sampling gears at any given site and time.

Materials and Methods

Study Site

The San Francisco Estuary, California, is a large, tidal estuary with extensive shallow-water shoals and bays bordering dredged navigation channels following the main axis of flow, and a novel mixture of native and non-native biota (Cohen and Carlton 1998). For this study, we sampled aquatic biota at two locations in the central region of the estuary, San Pablo Bay and Suisun Bay (Fig. 1), that were selected because they met specific physical criteria (detailed in “[Field Data Collection](#)”) and because longfin smelt have historically been abundant in these locations in autumn (Merz et al. 2013). We sampled in San Pablo Bay along the main navigational channel in October and November 2017 across day and night

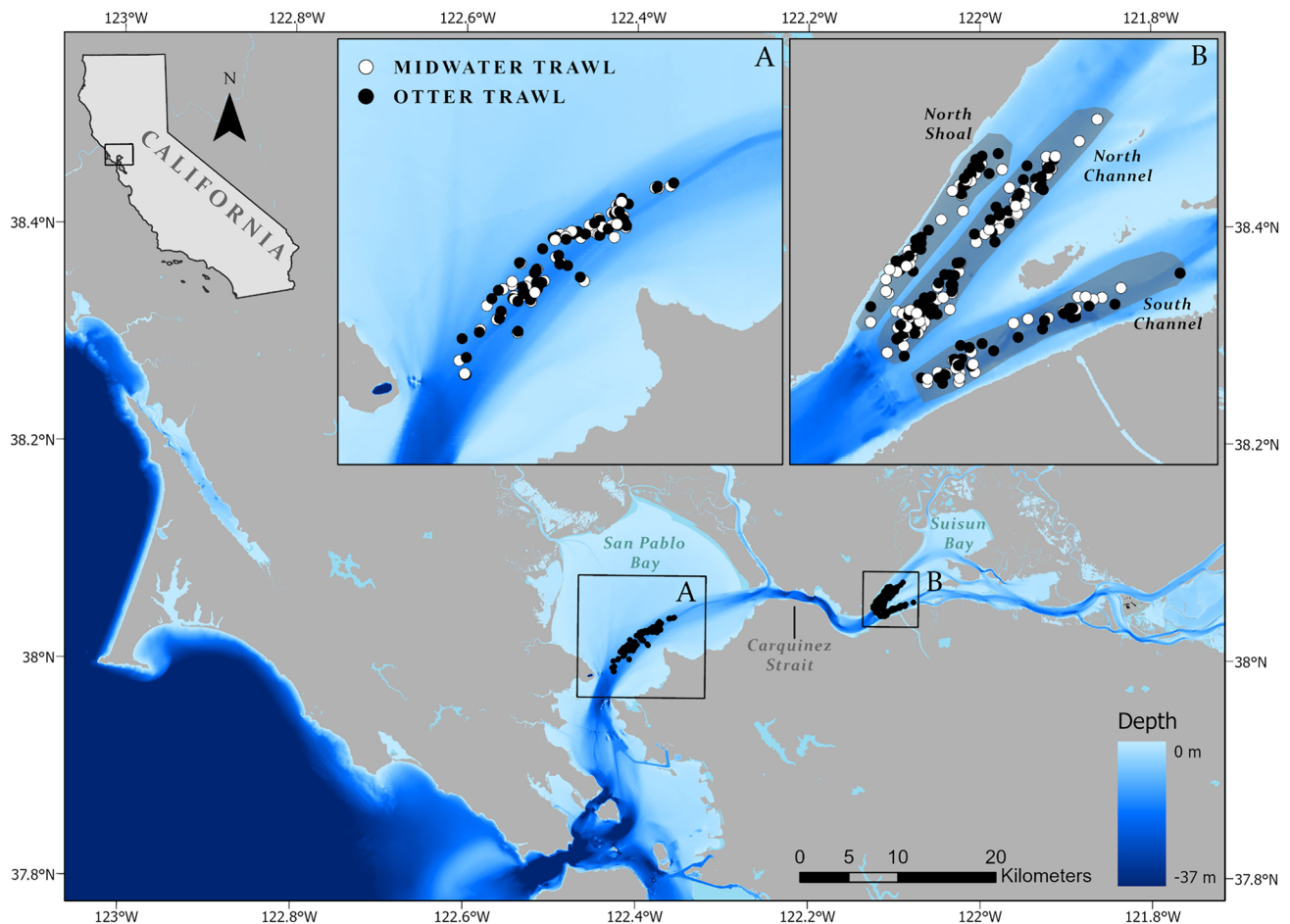


Fig. 1 Location of sampling sites in the San Francisco Estuary (**A** – San Pablo Bay sampled in 2017, **B** – Suisun Bay sampled in 2018). Point color corresponds to gear type (Midwater Trawl = Surface, Otter Trawl = Bottom) for each sampling event. Suisun Bay inset

(**B**) includes polygons for each lateral habitat sampled. Bathymetry is represented by the blue gradient, and bathymetry data were obtained from Fregoso et al. 2017

periods to examine whether diel phase and other factors influence vertical position of nekton (Question 1) based on species counts. San Pablo Bay was selected because it was sufficiently deep to discretely sample surface and bottom waters (depth mean \pm standard deviation, 13.3 ± 2.0 m). In the second year of our study (2018), we sampled in Suisun Bay to assess vertical position and integrated an assessment of the lateral (e.g., channels and peripheral shoals) position of nekton (Question 2). Nighttime data collection (and therefore diel phase) was dropped in the second year of sampling due to safety and logistical concerns.

We sampled in the downstream reaches of Suisun Bay in October and November 2018 to examine whether turbidity influences vertical and lateral positions of nekton (Question 2) based on species counts. This sampling took place in two navigation channels separated by an intertidal mudflat (north channel and south channel; sampled depth mean and standard deviation of 11.5 ± 0.8 m and 13.3 ± 1.7 m, respectively) and a shallow-water shoal (north shoal; 6.6 ± 0.9 m). We specifically

chose Suisun Bay because of the availability of deep channel and peripheral shallow shoal habitat in close proximity and high suspended sediment concentrations (Schoellhamer 2000). This allowed us to evaluate the effects of low light (as mediated by turbidity) and vertical and lateral positions. We assessed nekton distribution with respect to tidal variability (Question 3) using the data collected from both San Pablo and Suisun bays.

Field Data Collection

We examined the effects of diel phase on vertical position of nekton (Question 1) by conducting surface and demersal nekton sampling continuously during four 12.5-h periods in San Pablo Bay (Fig. 2). We sampled for one day and one night during both a spring tide and a neap tide to encompass the range of tidal variability during the study period. We used daytime surface and demersal sampling during a 2-week spring-neap tidal cycle in Suisun Bay (Fig. 2) to examine whether turbidity influences vertical and lateral positions (Question 2). Midwater

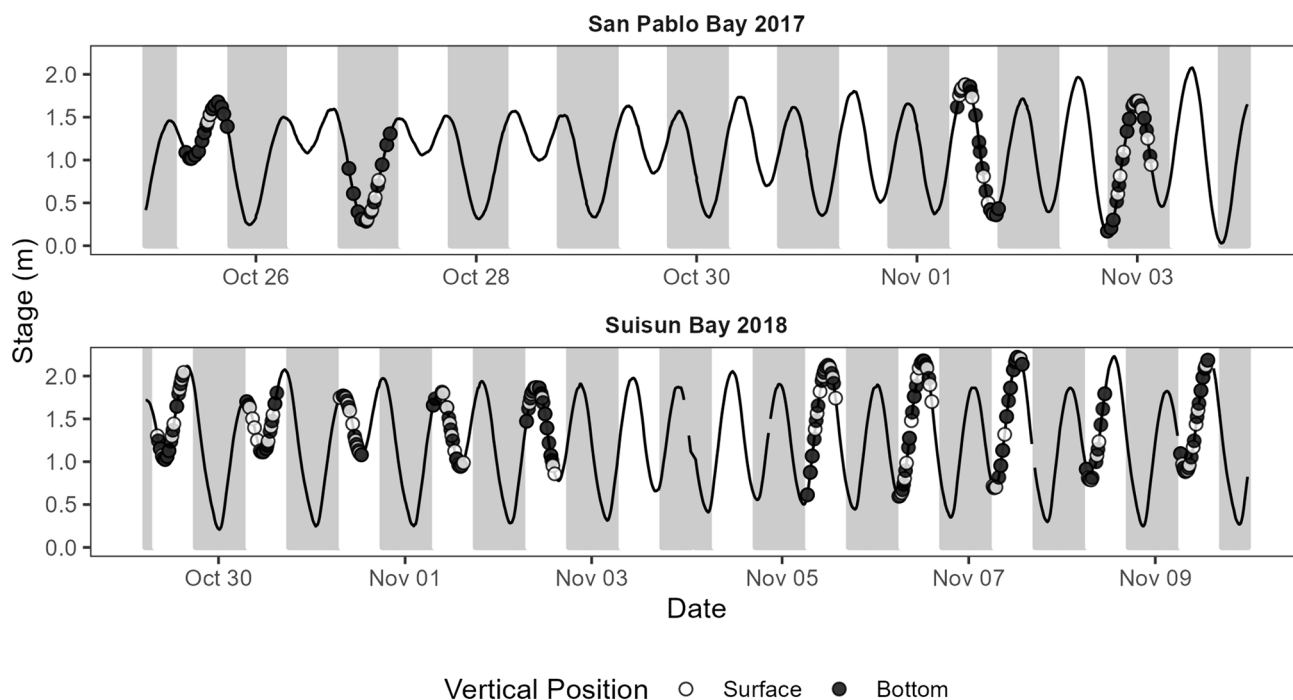


Fig. 2 Distribution of sampling events with respect to tidal stage and diel phase. Stage is represented by the line in each panel (obtained from <https://tidesandcurrents.noaa.gov>, NOAA 2022), and night by gray polygons. Sampling events are points, with vertical position

denoted by color (white - surface midwater trawls; black – bottom otter trawls). The top panel corresponds to San Pablo Bay sampling in 2017, and the bottom panel corresponds to Suisun Bay sampling in 2018

(surface) and otter (bottom) trawl specifications and deployment methods generally followed long-term fish monitoring programs in the San Francisco Estuary (Stompe et al. 2020; Tempel et al. 2021; Huntsman et al. 2022), specifically the San Francisco Bay Study (<https://wildlife.ca.gov/Conservation/Delta/Bay-Study>). The midwater trawl was 17.6 m long with a square mouth opening of 3.66 m in width and height and was towed at the surface. It had nine tapered panels ranging from 147-mm stretch mesh near the mouth to 13-mm stretch mesh in the cod end. The otter trawl was 5.3 m long with a mouth 4.8 m in width and 1.5 m in height. It had a 35-mm stretch mesh in the main body and was lined with a 6-mm stretch mesh cod end. We towed trawls at $\sim 3.5 \text{ km h}^{-1}$ for 15 min, but trawl speed varied slightly with gear type, prevailing currents, and environmental conditions.

During all trawls, we used a mechanical flowmeter (General Oceanics, Inc., Miami, FL, USA) to quantify water volume sampled by each trawl. To examine influences of diel phase and other factors on vertical position of nekton (Question 1), trawl paths were positioned in the center of the channel in San Pablo Bay. To examine influences of turbidity on vertical and lateral positions of nekton (Question 2), trawl paths were stratified by lateral position (north/south channel and north shoal) in Suisun Bay. We characterized water quality conditions at the time, place, and depth of each individual trawl sample with discrete measurements of

specific conductance ($\mu\text{S cm}^{-1}$), temperature ($^{\circ}\text{C}$), turbidity (formazin nephelometric units, FNU), dissolved oxygen concentration (mg l^{-1}), and chlorophyll concentration ($\mu\text{g l}^{-1}$) using a handheld YSI EXO2™ sonde (Yellow Springs Instruments, Yellow Springs, OH, USA). Individual fishes and invertebrates captured in trawls were identified to species and released on site.

Statistical Analysis

We characterized nekton-habitat relationships using Bayesian generalized linear mixed modeling, with the explicit goal of quantifying the effect of categorical factors (e.g., day/night and vertical and lateral positions) and continuous water quality variables on nekton counts. We selected nekton that were sufficiently abundant ($n > 25$ individuals for fish and $n > 200$ individuals for invertebrates) for subsequent count modeling to examine influences of diel phase and other factors on vertical position of nekton (Question 1) and influences of turbidity on vertical and lateral positions of nekton (Question 2). In most instances, nekton counts were overdispersed with many incidences of zero counts. To account for the possibility that zero counts reflect something other than species absence (i.e., incomplete detection), we used a zero-inflated negative binomial (ZINB) distribution for model formulation. Model structures were customized to address each question but were generally of the form

$$\begin{aligned}
 \text{Fish abundance} &\sim \text{Negative binomial}(\lambda_i, \rho) \\
 \log \lambda_i &= \log(\text{Effort}(\text{m}^3)_i) \\
 &+ \alpha_{\text{Random}[j]} + \beta_0 \\
 &+ \sum_j^{\text{cov}} \beta_{1j} \times \gamma_{1ij} \\
 &+ \sum_z^{\text{group}} \beta_{2z} \times \gamma_{2iz} \\
 \text{logit } \rho &= \Omega_0
 \end{aligned} \tag{1}$$

where λ_i is the count at site i and ρ is the “size parameter” or variance of the distribution. Effort was included as an offset term and is summarized as the volume of water sampled (m^3). α_{Random} represents a vector of study-specific random effects (j ; e.g., Julian day). β_0 represents the model intercept, β_1 represents a vector of slope coefficients associated with the vector of continuous variables (γ_{1i} ; e.g., specific conductance and turbidity) and associated intercepts, and β_2 represents a vector of slope coefficients associated with the vector of categorical variables (γ_{2i} ; e.g., day/night and surface/bottom) and associated intercepts. Models included a log link function for λ and a logit link for the zero-inflation component, which was assumed to have a constant probability across observations (Ω_0). All continuous variables were standardized by subtracting the mean and dividing by the standard deviation (z-score transformation).

To examine how diel phase and other factors influence vertical position, we modeled the effects of several explanatory variables on nekton counts (Question 1). Categorical variables included tide phase (four levels: ebb, flood, high slack, or low slack), diel phase (two levels: day or night), and vertical position (two levels: surface or bottom). Diel phase \times vertical position was included as an interaction term. Continuous variables included specific conductance and turbidity. Effort (volume) was included as an offset variable, and Julian day was included as a random effect to account for unmeasured variability associated with separate sampling days.

To examine how turbidity and other environmental factors influenced vertical and lateral positions, we modeled the effects of several explanatory variables on nekton counts (Question 2). Categorical variables included tide phase (four levels: ebb, flood, high slack, or low slack), vertical nekton position (two levels: surface or bottom), and lateral nekton position (three levels: shoal, north channel, or south channel). Vertical position \times lateral position was included as an interaction term. Consistent with our approach to Question 1, specific conductance and turbidity were included as continuous variables, effort was included as an offset variable, and Julian day was included as a random effect variable.

In models for examining Questions 1 and 2, we included tide as a categorical variable with four levels (ebb, flood,

high slack, or low slack) because this was deemed the approach with the least likelihood of overfitting models which already incorporate multiple predictors. Specific conductance covaries with the fluctuating estuarine salinity field, and further discretization of tide would result in substantial covariation with tide and specific conductance. With this approach, we are specifically assessing whether the direction of water movement influenced nekton distribution.

For statistical modeling, we used the “brms” package (Bürkner 2017) in the R statistical computing environment (R Core Team 2022). Fixed effects were assigned weakly informative ($\mu=0, \sigma=10$) normally distributed priors while random effects were assigned weakly informative ($\mu=0, \sigma=10$) Cauchy distributed priors. Models were implemented with four chains and iterated over 5000 times with a warm-up exceeding 1000 iterations. Step size was set to 0.99, and maximum tree depth was set to 15 to optimize the Hamiltonian Monte Carlo sampling dynamics.

Our goal with count modeling was to identify key predictors of abundance rather than to evaluate all possible combinations of covariates and identify the single best-fitting model. Thus, we identified a suite of 15 candidate models for each question based on combinations of categorical and continuous covariates that we deemed to have biological relevance. Models were compared using leave-one-out (LOO) cross validation from the loo package (Vehtari et al. 2022) to identify models with the best predictive performance. The Bayesian R^2 was calculated for each best-fitting model. If multiple models had a LOO model weight greater than zero, we used model averaging based on Bayesian stacking weights for subsequent model predictions, thus improving upon model fit from the best-fit model alone. We used Bayesian stacking weights to find an optimal model in the space spanned by all individual models from a predictive distribution close to the true data generating distribution; this method works well if there are multiple similar models (Yao et al. 2017). For model-averaged predictions, we combined all models that exhibited explanatory power above 10% of model weight (proportionally, 0.1), and then used this ensemble model to predict nekton densities with respect to covariates. Although we acknowledge that gear efficiency is different between trawl types (Huntsman et al. 2022), sampling across different environmental conditions allows us to interpret observed variability as a function of the centroid of a species’ distribution within the water column.

Comparisons across multiple gear types can be biased from differences in catchability across gears (i.e., midwater trawl and otter trawl). Catchability is a function of the probability that an individual is available to the sampling gear, and the probability that an individual is retained by the sampling gear if available (i.e., gear efficiency; Walsh 1991). Relative catchability has been evaluated for species

and gear types modeled in this study (Huntsman et al. 2022), although actual estimates of gear efficiency exist for only a few species and are size-dependent (Mitchell et al. 2017; Mitchell and Baxter 2021). For example, retention for fishes commonly sampled by the midwater trawl (American shad *Alosa sapidissima*, threadfin shad) exceeds 95% at sizes longer than 45 mm fork length (Mitchell and Baxter 2021). Given that mean sizes for these and other modeled species from this study exceeded that threshold, we assume that differences in catchability across our gear types are tied primarily to availability. Thus, even if our density values may be influenced by catchability, results likely reflect actual distributional differences in space.

For a higher-resolution evaluation of vertical or lateral changes in nekton position with respect to tidal variability (Question 3), we normalized tide stage (water elevation relative to mean lower low water) so that low slack tide is 0, high slack tide is 1, and intermediate values represent a percentage of high tide as described in Colombano et al. (2020). Because nearby velocity or flow data were not available for both sampling regions, we used tidal stage as an approximation. Following this approach, water elevation data were ultimately classified into eight categories based on tide stage: low slack, early flood, peak flood, late flood, high slack, early ebb, peak ebb, and late ebb. For this analysis, flood corresponds to ascending tidal stage, and ebb corresponds to descending tidal stage. This differs from other definitions of flood and ebb that are derived from increasing or decreasing velocity/flow, metrics not available at our study sites. For each tide category, we plotted the proportion of individuals of a given species that were captured in each vertical (surface or bottom) or lateral (channel or shoal) position. We summarize distributional data proportionally, rather than total catch, to minimize the impact of unequal sample sizes

(either number of tows or individuals captured) on interpretation of relative nekton distribution. With this approach, we specifically assess the effect of position within a tidal cycle on the vertical or lateral distribution of nekton.

Results

We collected 330 trawl samples across a wide range of environmental conditions, although logistical constraints prevented equal sample sizes across all studied categorical factors (Table 1, Supplemental Fig. S1). Specific conductance ranged from 30,934 to 45,033 $\mu\text{S cm}^{-1}$ in San Pablo Bay and ranged from 19,352 to 33,771 $\mu\text{S cm}^{-1}$ in Suisun Bay. Specific conductance was slightly higher at the bottom of the water column in both regions (Table 1). Salinity, as estimated from specific conductance, ranged from 21.0 to 29.2 practical salinity units (PSU) in San Pablo Bay and from 11.6 to 21.2 PSU in Suisun Bay. Turbidity ranged from 0 to 44.7 FNU in San Pablo Bay and from 4.3 to 100.0 FNU in Suisun Bay and was also higher at the bottom of the water column (Table 1). Measured temperatures (San Pablo Bay, 14.9–17.4 °C; Suisun Bay, 15.3–18.6 °C) remained below 22 °C, which represents a potential threshold limiting the distribution of adult longfin smelt (U.S. Fish and Wildlife Service 2023). Concentrations of dissolved oxygen (San Pablo Bay, 6.8–8.3 mg l^{-1} ; Suisun Bay, 7.3–8.4 mg l^{-1}) were not low enough to be considered hypoxic ($< 5 \text{ mg l}^{-1}$), and concentrations of chlorophyll *a* (San Pablo Bay, 0.7–8.6 $\mu\text{g l}^{-1}$; Suisun Bay, 0.1–6.6 $\mu\text{g l}^{-1}$) remained consistently low. Therefore, temperature, dissolved oxygen concentration, and chlorophyll *a* concentration were excluded from further modeling to simplify model selection.

Table 1 Sampling effort (total number of trawls, N) in each study for each question/region and vertical habitat (Surface = Midwater Trawl, Bottom = Otter Trawl), with a summary of the corresponding water quality conditions (min-max, mean \pm standard deviation)

	Surface		Bottom	
	Min-max	Mean \pm SD	Min-max	Mean \pm SD
Question 1, San Pablo Bay	N = 51		N = 54	
Temperature (°C)	15.0–17.4	15.9 \pm 0.5	14.9–16.2	15.5 \pm 0.3
Salinity (PSU)	21.0–28.6	25.1 \pm 1.9	23.1–29.2	26.7 \pm 1.5
Specific conductance ($\mu\text{S cm}^{-1}$)	30934–44242	38679 \pm 3089	34345–45033	41473 \pm 2306
Turbidity (FNU)	0.0–11.3	3.5 \pm 3.8	1.9–44.7	9.1 \pm 7.8
Dissolved oxygen (mg l^{-1})	7.1–8.3	7.5 \pm 0.3	6.8–7.5	7.1 \pm 0.2
Chlorophyll <i>a</i> ($\mu\text{g l}^{-1}$)	0.8–8.6	3.6 \pm 1.7	0.7–3.8	2.7 \pm 0.5
Question 2, Suisun Bay	N = 113		N = 112	
Temperature (°C)	15.3–18.6	17.0 \pm 0.6	16.0–17.4	17.1 \pm 0.3
Salinity (PSU)	11.6–21.2	15.6 \pm 2.1	13.2–21.2	17.5 \pm 2.0
Specific conductance ($\mu\text{S cm}^{-1}$)	19352–33653	25422 \pm 3239	21837–33771	28313 \pm 3033
Turbidity (FNU)	4.3–37.7	9.4 \pm 4.5	6.2–100.0	26.8 \pm 19.7
Dissolved oxygen (mg l^{-1})	7.4–8.4	7.9 \pm 0.2	7.3–8.3	7.9 \pm 0.2
Chlorophyll <i>a</i> ($\mu\text{g l}^{-1}$)	0.4–6.6	1.5 \pm 0.8	0.1–3.5	1.1 \pm 0.7

In total, 29 fish species (3494 individuals) and 3 caridean shrimp species (12,314 individuals) were observed in trawl samples (Table 2). In San Pablo Bay, we captured 20 fish species (1987 individuals), and in Suisun Bay, we captured 18 fish species (1507 individuals). Longfin smelt comprised 2% of our total fish catch, with 26 individuals observed in San Pablo Bay and 45 individuals in Suisun Bay. Northern anchovy, American shad, and plainfin midshipman *Porichthys notatus* were the three most abundant fish species, comprising 57%, 20%, and 7% of total fish catch, respectively. No fish species exhibited clear evidence for multiple abundant cohorts, and most sampled individuals among all species were < 100 mm standard length (Supplemental Fig. S2). California bay shrimp (*Crangon franciscorum*) was the most abundant invertebrate species and comprised 81% of the invertebrate catch.

Question 1: How Does Diel Phase Influence Vertical Distribution of Nekton?

Longfin smelt, northern anchovy, plainfin midshipman, American shad, and the caridean shrimp *C. franciscorum* were included for subsequent modeling with 15 a priori candidate models (Table 3). Model selection indicated three to five models comprising greater than 10% of model weight for each species (Table 3). Bayesian R^2 values ranged between 0.07 and 0.51 for the best fit models for each species. Diel phase and vertical position were important for explaining modeled densities for all species, but the relative impacts of these factors differed by species (Supplemental Fig. S3). Longfin smelt, American shad, plainfin midshipman, and *C. franciscorum* were observed in higher densities at the bottom of the water column irrespective of diel phase (Fig. 3), with the strongest effect of vertical position on plainfin midshipman and *C. franciscorum*. American shad, plainfin midshipman, and *C. franciscorum* were observed in higher densities at night irrespective of vertical position, with American shad showing the strongest relative response to diel phase. Northern anchovy were affected by the interaction between vertical position and diel phase, with higher densities caught at the surface at night and with similar densities captured throughout the water column during daylight hours. No other interactions between vertical position and diel phase were observed. The relative effect of diel phase on northern anchovy at the surface was the strongest influence of diel phase observed among all five species. Associations between densities and modeled water quality variables were uncommon. Longfin smelt and northern anchovy were positively associated with specific conductance (Supplemental Fig. S3), *C. franciscorum* were positively associated with turbidity (Supplemental Fig. S3), and no other species exhibited associations with either specific conductance or turbidity.

Question 2: How Do Environmental Conditions Influence Vertical and Lateral Distribution of Nekton?

Longfin smelt, American shad, northern anchovy, striped bass, Shokihaze goby *Tridentiger barbatus*, threadfin shad, yellowfin goby *Acanthogobius flavimanus*, and all three caridean shrimp collected in Suisun Bay (*C. franciscorum*, *Palaemon macrodactylus*, *Palaemon modestus*) were included for subsequent modeling with 15 a priori candidate models (Table 3). Model selection indicated overlap in multiple models for each species, with between two and six models comprising greater than 10% of model weight (Table 3). Bayesian R^2 values ranged between 0.24 and 0.53 for the best fit models for each species. Models including lateral position and vertical position were important for explaining densities for all fish and invertebrate species, although relative impacts differed (Supplemental Fig. S4). Densities of all taxa were higher on the shoal than in either the north or south channel habitat (Fig. 4). Densities of northern anchovy, American shad, and threadfin shad were all higher at the surface, and densities of longfin smelt, striped bass, Shokihaze goby, yellowfin goby, and all three shrimp species were higher at the bottom of the water column (Fig. 4).

In Suisun Bay, many species had associations with specific conductance and turbidity (Table 3, Fig. 5, Supplemental Fig. S4). Longfin smelt and northern anchovy were positively associated with specific conductance (Fig. 5). American shad, threadfin shad, striped bass, *P. modestus*, and *P. macrodactylus* were negatively associated with specific conductance (Fig. 5), with threadfin shad exhibiting the strongest negative association. Shokihaze goby, yellowfin goby, and *C. franciscorum* were weakly associated with specific conductance. Longfin smelt were positively associated with turbidity at the surface, but the association between longfin smelt and turbidity was negligible at the bottom of the water column (Fig. 5). Northern anchovy, American shad, and threadfin shad were negatively associated with turbidity. Shokihaze goby and all three shrimp species were positively associated with turbidity. Striped bass were positively associated with turbidity at the surface and negatively associated with turbidity at the bottom of the water column. Yellowfin goby had a weak relationship with turbidity.

Question 3: Is There Evidence for Vertical or Lateral Changes in Nekton Distribution with Respect to Tidal Variability?

Samples were collected across all discretized tidal phases in 2017 (San Pablo Bay), but the number of tows during each tide phase varied consistently with the duration of the tide phase. There was mixed evidence for variability in vertical

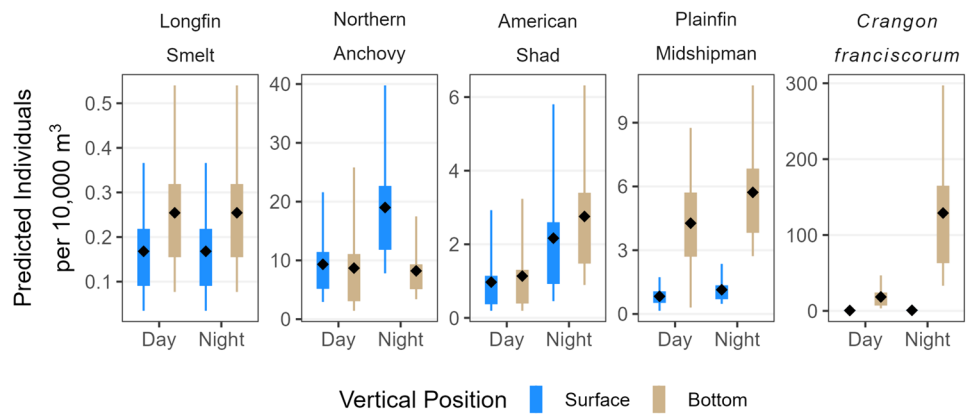
Table 2 Summary of fishes and invertebrates collected in this study. Table includes total count of fishes and invertebrates, and percentage of total collected in each region and vertical habitat (Surface = Midwater Trawl, Bottom = Otter Trawl). Species included for count models are noted with a superscript (a) for Question One and (b) for Question Two

	Latin binomial	Question 1				Question 2				Total	
		San Pablo Bay (2017)				Suisun Bay (2018)					
		Surface		Bottom		Surface		Bottom			
		n	%	n	%	n	%	n	%	n	%
Fish species											
Northern anchovy ^{a,b}	<i>Engraulis mordax</i>	703	82	777	67	481	41	35	9	1996	57
American shad ^{a,b}	<i>Alosa sapidissima</i>	76	9	37	3	561	48	17	5	691	20
Plainfin midshipman ^a	<i>Porichthys notatus</i>	32	4	217	19	0	0	9	2	258	7
Striped bass ^b	<i>Morone saxatilis</i>	15	2	8	1	47	4	87	23	157	4
Shokihaze goby ^b	<i>Tridentiger barbatus</i>	0	0	10	1	0	0	129	34	139	4
Longfin smelt ^{a,b}	<i>Spirinchus thaleichthys</i>	5	1	21	2	5	0	40	11	71	2
Unknown larval fish		0	0	44	4	4	0	0	0	48	1
Threadfin shad ^b	<i>Dorosoma petenense</i>	2	0	0	0	35	3	0	0	37	1
Yellowfin goby ^b	<i>Acanthogobius flavimanus</i>	0	0	5	0	0	0	30	8	35	1
Jacksmelt	<i>Atherinopsis californiensis</i>	5	1	0	0	4	0	0	0	9	0
California halibut	<i>Paralichthys californicus</i>	0	0	8	1	0	0	0	0	8	0
Pacific staghorn sculpin	<i>Leptocottus armatus</i>	0	0	0	0	0	0	8	2	8	0
Speckled sanddab	<i>Citharichthys stigmaeus</i>	0	0	6	1	0	0	0	0	6	0
Shimofuri goby	<i>Tridentiger bifasciatus</i>	0	0	0	0	0	0	4	1	4	0
River lamprey	<i>Lampetra ayresii</i>	0	0	2	0	0	0	1	0	3	0
Unknown fish		0	0	1	0	1	0	1	0	3	0
Brown smoothhound	<i>Mustelus henlei</i>	0	0	2	0	0	0	0	0	2	0
Starry flounder	<i>Platichthys stellatus</i>	0	0	0	0	0	0	2	1	2	0
Brown rockfish	<i>Sebastes auriculatus</i>	0	0	2	0	0	0	0	0	2	0
English sole	<i>Parophrys vetulus</i>	0	0	2	0	0	0	0	0	2	0
Sacramento splittail	<i>Pogonichthys macrolepidotus</i>	0	0	0	0	1	0	1	0	2	0
Sand sole	<i>Psettichthys melanostictus</i>	0	0	2	0	0	0	0	0	2	0
Pacific halibut	<i>Hippoglossus stenolepis</i>	0	0	0	0	0	0	1	0	1	0
Arrow goby	<i>Clevelandia ios</i>	0	0	1	0	0	0	0	0	1	0
Chameleon goby	<i>Tridentiger trigonocephalus</i>	0	0	0	0	0	0	1	0	1	0
Cheekspot goby	<i>Ilypnus gilberti</i>	0	0	1	0	0	0	0	0	1	0
Green sturgeon	<i>Acipenser medirostris</i>	0	0	0	0	0	0	1	0	1	0
Slender sole	<i>Lyopsetta exilis</i>	0	0	1	0	0	0	0	0	1	0
Topsmelt	<i>Atherinops affinis</i>	1	0	0	0	0	0	0	0	1	0
Threes-pined stickleback	<i>Gasterosteus aculeatus</i>	1	0	0	0	0	0	0	0	1	0
White sturgeon	<i>Acipenser transmontanus</i>	0	0	0	0	0	0	1	0	1	0
Invertebrates											
California bay shrimp ^{a,b}	<i>Crangon franciscorum</i>	8	33	1867	84	4	25	8332	81	10,211	81
Siberian prawn ^b	<i>Palaemon modestus</i>	0	0	0	0	7	44	906	9	913	7
Migrant prawn ^b	<i>Palaemon macrodactylus</i>	0	0	0	0	1	6	862	8	863	7
Unknown shrimp	Decapoda	0	0	327	15	0	0	0	0	327	3
Dungeness crab	<i>Cancer magister</i>	0	0	0	0	1	6	112	1	113	1
Harris mud crab	<i>Rhithropanopeus harrisi</i>	0	0	0	0	0	0	1	0	1	0
Unknown jellyfish		16	67	8	0	3	19	7	0	34	0
Brackish-water corbula	<i>Potamocorbula amurensis</i>	0	0	9	0	0	0	105	1	114	1

Table 3 Candidate models for each species for each study question. Model weights are based on Bayesian stacking weights for each individual species modeled. Modeled variables include the categorical factors vertical position (Vertical), diel phase (Diel), lateral position (Lateral), and tide phase (Tide), and the continuous variables specific conductance and turbidity. The random effect of Julian day was included in each model, and was the only variable included in model 1. Candidate models that exceeded the 0.1 proportional model weight threshold for model averaging are italicized. Bayesian R² values are included for the best fitting model for each species (denoted by asterisk)

Question	Model no	Modeled variables	Model weights (stacking)														
			Longfin smelt	Northern anchovy	American shad	Plainfin midshipman	Striped bass	Shokihaze goby	Threadfin shad	Yellowfin goby	<i>Crangon franciscorum</i>	<i>Palaeomon modestus</i>	<i>Palaeomon macrondactylus</i>				
1	1	Random effect only	0	<i>0.11</i>	0	0	0	0	0	0	0	0	0	0	0	0	
	2	Vertical	<i>0.46*</i>	0	0	<i>0.52*</i>	0	0	0	0	0	0	0	0	0	0	
	3	Diel phase	0	<i>0.11</i>	<i>0.19</i>	0	0	0	0	0	0	0	0	0	0	0	0
	4	Specific conductance	<i>0.36</i>	0	0	0	0	0	0	0	0	0	0	0	0	0	0
	5	Turbidity	0	0	0	<i>0.18</i>	0	0	0	0	0	0	0	0	0	0	0
	6	Tide	0	0	<i>0.24</i>	0	0	0	0	0	0	0	0	0	0	0	0
	7	Vertical X diel	<i>0.06</i>	0	0	0	0	0	0	0	0	0	0	0	0	0	0
	8	Vertical X turbidity	0	0	0	<i>0.05</i>	0	0	0	0	0	0	0	0	0	0	0
	9	Vertical X tide	0	0	0	0	0	0	0	0	0	0	0	0	0	0	0
	10	Vertical + SC	0	0	0	0	0	0	0	0	0	0	0	0	0	0	0
	11	Diel phase + SC	0	0	0	0	0	0	0	0	0	0	0	0	0	0	0
	12	Vertical X diel + SC	<i>0.12</i>	<i>0.30</i>	0	0	0	0	0	0	0	0	0	0	0	0	0
	13	Vertical X diel + turbidity	0	0	0	0	0	0	0	0	0	0	0	0	0	0	0
	14	Diel X tide	0	0	0	0	0	0	0	0	0	0	0	0	0	0	0
	15	Vertical X diel X tide	0	<i>0.48*</i>	<i>0.57*</i>	<i>0.26</i>	0	0	0	0	0	0	0	0	0	0	0
Bayesian R ²			<i>0.07</i>	<i>0.20</i>	<i>0.21</i>	<i>0.32</i>	0	0	0	0	0	0	0	0	0	0	
2	1	Random effect only	0	0	0	0	0	0	0	0	0	0	0	0	0	0	0
	2	Vertical	0	0	<i>0.02</i>	0	0	0	0	0	0	0	0	0	0	0	0
	3	Lateral	<i>0.03</i>	0	0	0	0	0	0	0	0	0	0	0	0	0	0
	4	Specific conductance	0	0	0	0	0	0	0	0	0	0	0	0	0	0	0
	5	Turbidity	0	0	0	0	0	0	0	0	0	0	0	0	0	0	0
	6	Tide	0	0	0	0	0	0	0	0	0	0	0	0	0	0	0
	7	Vertical X lateral	0	<i>0.02</i>	<i>0.02</i>	0	0	0	0	0	0	0	0	0	0	0	0
	8	Vertical X turbidity	0	<i>0.03</i>	<i>0.02</i>	0	0	0	0	0	0	0	0	0	0	0	0
	9	Vertical X tide	<i>0.07</i>	0	<i>0.14</i>	0	0	0	0	0	0	0	0	0	0	0	0
	10	Vertical X lateral + turbidity	0	<i>0.02</i>	0	0	0	0	0	0	0	0	0	0	0	0	0
	11	Vertical X lateral + SC	<i>0.33</i>	<i>0.14</i>	<i>0.01</i>	0	0	0	0	0	0	0	0	0	0	0	0
	12	Vertical X lateral + turbidity + SC	0	<i>0.21</i>	<i>0.33</i>	0	0	0	0	0	0	0	0	0	0	0	0
	13	Vertical X turbidity + lateral	<i>0.57*</i>	<i>0.03</i>	0	0	0	0	0	0	0	0	0	0	0	0	0
	14	Lateral X tide	0	0	0	0	0	0	0	0	0	0	0	0	0	0	0
	15	Vertical X lateral X tide	0	<i>0.55*</i>	<i>0.46*</i>	0	0	0	0	0	0	0	0	0	0	0	0
Bayesian R ²			<i>0.24</i>	<i>0.28</i>	<i>0.45</i>	0	0	0	0	0	0	0	0	0	0	0	

Fig. 3 Ensemble predicted densities of modeled nekton with respect to vertical position (as assessed by surface and bottom trawls) and diel phase (Question 1, San Pablo Bay 2017). Point represents the mean, thick line represents 50% credible intervals around the mean, and the thin line represents 90% credible intervals around the mean



position associated with tide phase (Fig. 6). During the day, low catches across many tide phases made vertical position difficult to ascertain for the pelagic northern anchovy and American shad. Demersally oriented plainfin midshipman and *C. franciscorum* were caught at the bottom during all tides. At night, the proportions of northern anchovy and American shad were higher at the surface at early flood peak flood; high, early ebb; and late ebb tides. Plainfin midshipman were rarely observed at the surface, but when it happened, it was most frequently at night on early flood, peak flood, and late flood tide.

In 2018 (Suisun Bay), logistical constraints prevented sample collection during one discretized tide period (early ebb), and shoal samples were not collected with the otter trawl at peak ebb (Fig. 7). Northern anchovy and American shad exhibited the strongest evidence for variability in lateral position associated with tidal cycles. Northern anchovy were in

higher proportion on the shoal at high and ebb tide, and in higher proportion in the channel on low and peak flood tides. The proportion of American shad in the channel increased through flood tide, peaking at high tide, and then declined on ebb tide. The proportions of Shokihaze and yellowfin gobies were highest on the shoal. Longfin smelt were mostly associated with the shoal except for four individuals captured in the channel at ebb tide. Striped bass were also mostly associated with the shoal except during early flood tide and at high tide. *C. franciscorum* distribution was variable across tides and was highest in the channel on early flood and high tide. *P. macrodactylus* and *P. modestus* were only associated with the channel at high tide. By looking at the relative distribution of taxa across habitat tide, we inherently incorporate both the hydrodynamic effects of tide (current direction, velocity, stage) and fluctuations in the estuarine gradient. This can be observed in changes in nekton catch across a tidal cycle. For

Fig. 4 Ensemble predicted densities of modeled nekton with respect to vertical position (as assessed by surface and bottom trawls) and lateral position (Question 2; Suisun Bay 2018). Point represents the mean, box represents 50% credible intervals around the mean, and the thin line represents 90% credible intervals around the mean

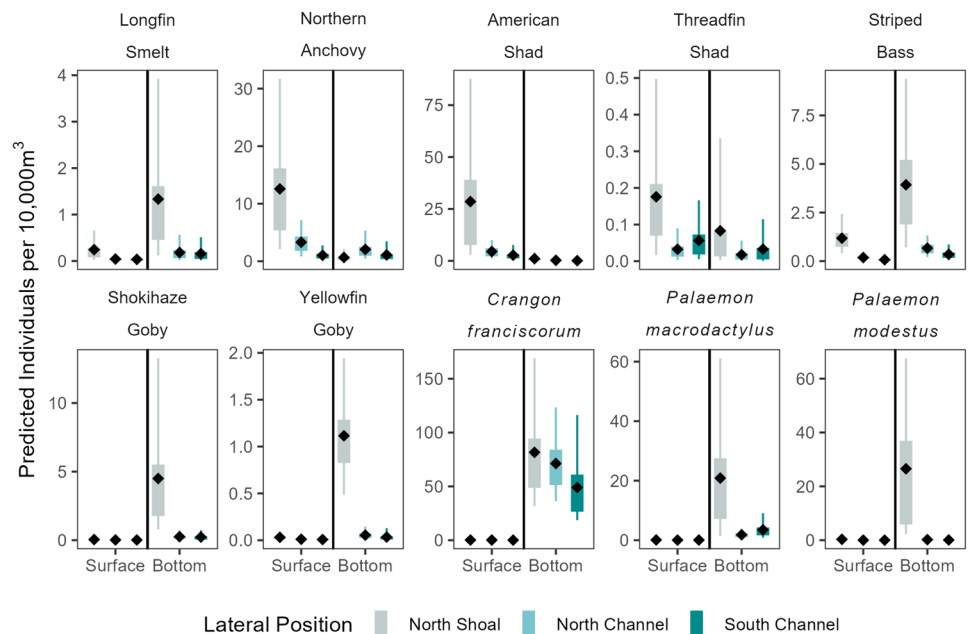
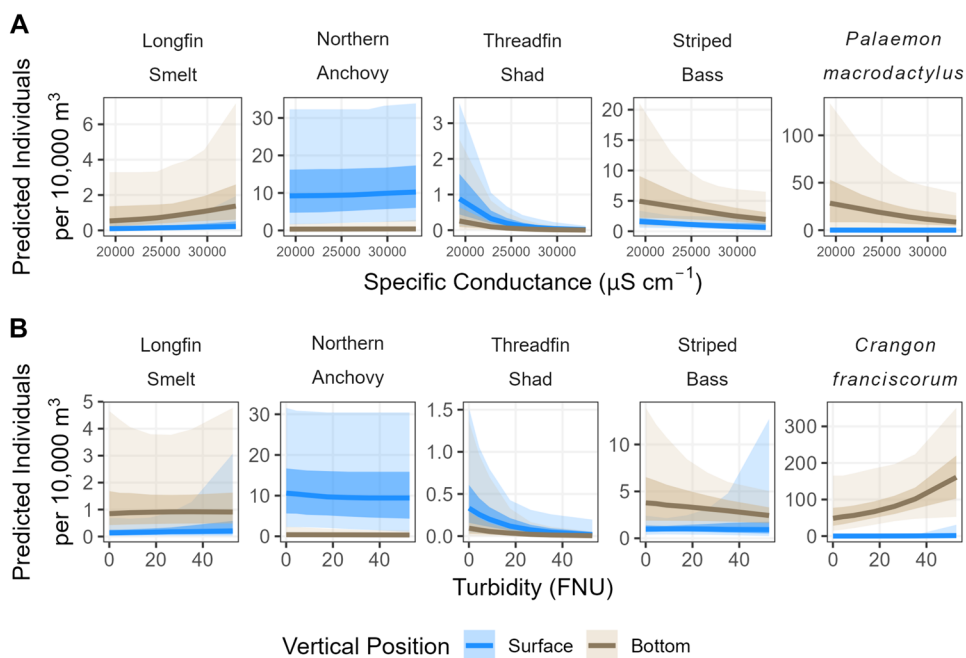


Fig. 5 Ensemble predicted densities of a subset of modeled nekton with respect to vertical position (as assessed by surface and bottom trawls) and continuous environmental variables (**A** – specific conductance; **B** – turbidity) based on Question 2 (Suisun Bay 2018). Line represents the median, dark shading represents 50% credible intervals around the mean, and lighter shading represents 90% credible intervals around the mean. Not all relationships with continuous variables are shown because the relative impacts of some continuous variables may be slight due to those models having low model weight (see Table 3)



example, northern anchovy and longfin smelt were caught in highest numbers during late flood tide, and threadfin shad and striped bass were caught in highest numbers around low tide.

Discussion

We documented clear variability in sampled densities of nekton species across diel phase (day/night), vertical position (surface/bottom), and lateral position (channel/shoal). There was also evidence for species-specific differences in

vertical or lateral distribution associated with tidal variability and turbidity. Specific conductance was also an important predictor for many species and will be discussed in “Salinity and Turbidity” with respect to the underlying estuarine salinity gradient. Longfin smelt were infrequently observed but were most commonly encountered near the bottom of the water column and in shoal habitats, with increased catch in low light conditions (e.g., at night or under elevated turbidity). Altogether, there was substantial variability in the direction and magnitude of the response of each species to studied habitat elements. Collectively, these species-specific

Fig. 6 Proportion of individuals in each vertical position during a given tide phase in 2017 (San Pablo Bay). Colored bars represent the vertical position, and the black line signifies an idealized representation of tide stage. Number of individuals collected for each tide phase is noted above each colored bar, with gray bars denoting relative catch. Tide phases where zero individuals were caught are blank

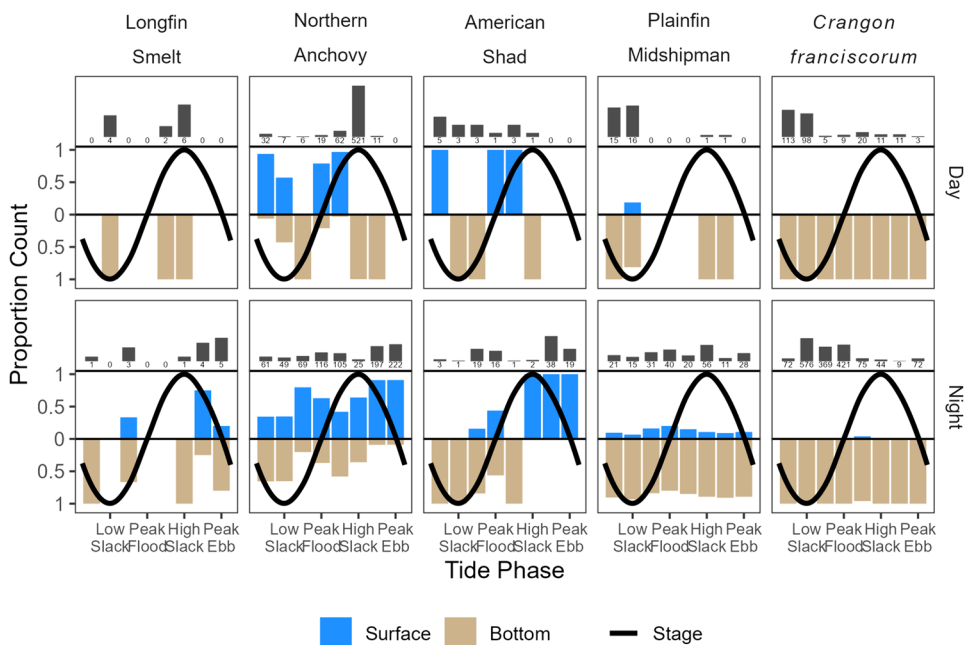
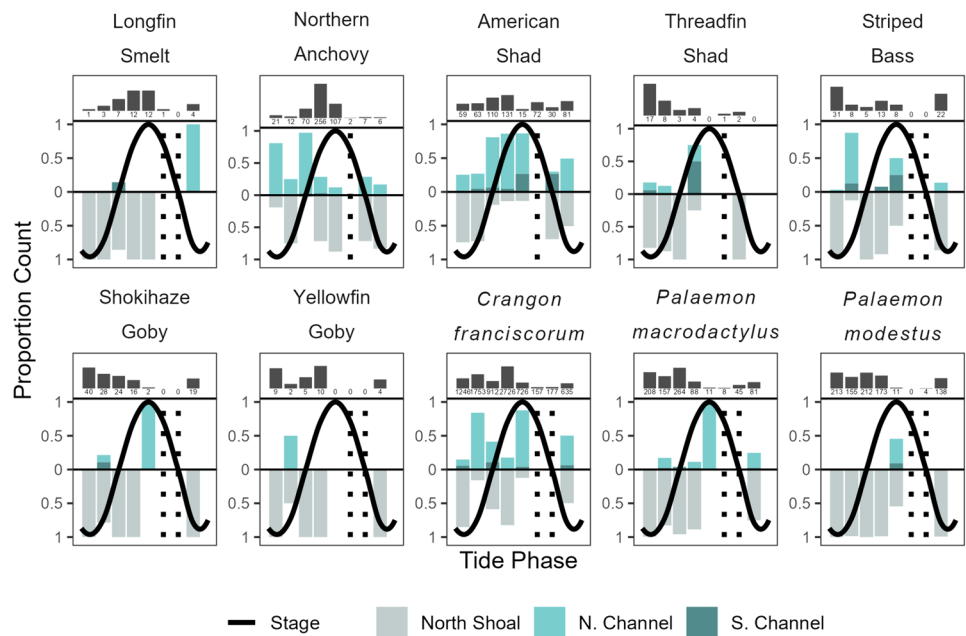


Fig. 7 Proportion of individuals captured in a sampled habitat during a given tide phase in 2018 (Suisun Bay). Colored bars represent the specific habitats, and the black line signifies an idealized representation of tide stage that corresponds with the tide phases depicted by each bar. Number of individuals collected for each tide phase is noted above each bar, with upper gray bars denoting catch of each species. Tide phases where zero individuals were caught are blank, and tide phases where no shoal samples were collected are filled by a dotted line. Northern Anchovy, American Shad, and Threadfin Shad counts are based on mid-water trawl (surface) data, and all other species are based on otter trawl (bottom) data



habitat associations provide insight into factors influencing the distribution of nekton and thus the vulnerability of individual species to detection by sampling gears at different times and locations.

Diel Phase and Vertical Position

Nekton densities were influenced by diel phase, with higher densities of most species at night. However, not all species exhibited consistent responses near the surface and near the bottom, highlighting species-dependent effects of diel phase. There were notable differences between American shad and the other two pelagic fish, northern anchovy and longfin smelt. While American shad densities were higher at night throughout the water column, northern anchovy densities were only higher at night at the surface, indicating upward vertical migration at night. Diel vertical migration is observed in many pelagic fish species (Neilson and Perry 1990; Mehner 2012) and can reflect fish following diel vertical migration by zooplankton prey (e.g., Bollens and Frost 1989) or anti-predator behavior (e.g., Scheuerell and Schindler 2003). Northern anchovy consume zooplankton (Koslow 1981), which are known to make diel vertical migrations in open waters of the San Francisco Estuary (Kimmerer et al. 1998), indicating that the vertical movements observed in this study may be foraging-related. However, it is also possible that predator avoidance is an important driver in microhabitat selection. As visibility declines at night or during other low-light conditions, trawl capture efficiency can increase for some species because the net is harder to see (Walsh 1991). This is most likely for species which we observed at higher densities at night throughout

the water column, such as American shad, plainfin midshipman, and *C. franciscorum*.

Modeled densities of longfin smelt across vertical position (surface or bottom) did not differ across day and night periods, although this species can exhibit substantial diel vertical migration associated with prey movements in other systems (Chigbu et al. 1998). Our findings may be related to the overall low density of longfin smelt encountered in this study, as only 26 individuals were encountered during sampling for this question (diel phase and vertical position). Although diel phase was not important based on model predictions, catches of longfin smelt at the surface only occurred at night (a total of five individuals), with zero longfin smelt encountered at the surface during the day. The presence of longfin smelt at the surface at night is consistent with diel vertical migrations observed in Lake Washington, where juvenile and adult fish are largely absent from shallow waters during the day and are found higher in the water column during low light periods (dusk and night) in autumn (Quinn et al. 2012). Based on the discrepancy between our statistical results (possibly due to few numbers of individuals) and findings from other regions (Chigbu et al. 1998; Quinn et al. 2012), a further study of diel vertical migration by longfin smelt in the San Francisco Estuary could help verify our observations. Our assessment of diel phase is limited by sampling in 1 year in one location, and a further study could help further refine the relative quantitative impacts across nekton species.

While longfin smelt and striped bass densities were higher at the bottom of the water column, American shad and threadfin shad densities were higher at the surface, which has implications for the relative influence of tide on

distribution, as surface water velocities can be higher (see “Lateral and Vertical Positions”). Similarly, the higher density of northern anchovy at the bottom of the channel could be related to vertical differences in water velocity, channel salinity and turbidity associated with localized gravitational circulation (Schoellhamer 2000), or some other influence of tidal currents.

Lateral and Vertical Positions

Shallow-water habitats often support different nekton assemblages and densities than deeper channels through various mechanisms, including depth-mediated habitat elements such as vegetation (Thayer and Chester 1989), distribution of prey (Bottom and Jones 1990), and refuge from predators (Paterson and Whitfield 2000) or water velocity (Feyrer et al. 2013). In contrast with our limited observations, longfin smelt densities have historically been slightly higher in the channel than on the shoal (Rosenfield and Baxter 2007), with lateral shifts not noted in the literature. However, there is substantial evidence for use of other shallow-water habitats at various life stages throughout the San Francisco Estuary (Grimaldo et al. 2017; Lewis et al. 2020; Barros et al. 2022). Longfin smelt densities were higher at the bottom of the water column in the channel and the shoal, consistent with other sampling in this study and other regions (Chigbu et al. 1998; Quinn et al. 2012). Striped bass densities were also higher at the bottom of the water column and on the shoal, consistent with Sommer et al. (2011), who postulated an estuary-wide shift of striped bass away from the channel toward the shoal and systematic undersampling of striped bass by surface-water sampling methods (i.e., midwater trawls). Shokihaze and yellowfin gobies were more abundant at the bottom and on the shoal, consistent with their demersal behavior and known shallow-water preferences (Moyle 2002).

Shrimp comprised approximately 78% of total catch in this study, but despite their relative abundance, little is known about the specific habitat associations of shrimp species in open-water habitats of the San Francisco Estuary. Shrimp lateral distributions were consistent with other studies which have indicated littoral distributions of *P. macrodactylus* and *P. modestus* (Young et al. 2017) and more even distribution of *C. franciscorum* (Siegfried 1980; Hatfield 1985; Brown and Hieb 2014). Despite the potential for niche displacement or exclusion of the native *C. franciscorum* by non-native *Palaemon* sp., habitat partitioning suggests the possibility of coexistence, with native (*C. franciscorum*) and non-native (*P. macrodactylus*, *P. modestus*) species. This coexistence has been documented between non-native *P. macrodactylus* and other caridean shrimps in several European estuaries (Berglund 1982; González-Ortegón et al. 2010; Kuprijanov et al. 2017).

Salinity and Turbidity

Salinity is an important driver of nekton distribution in estuaries, and it is an important expression of dynamic habitat that fluctuates with tidal and hydrologic variability (Greenwood 2007; Feyrer et al. 2015). Striped bass, threadfin shad, northern anchovy, and longfin smelt exhibited the strongest associations with salinity on the tidal timescales evaluated in this study, which likely demonstrates their relative mobility and movements associated with the tidally fluctuating salinity field. Northern anchovy and longfin smelt had positive associations with salinity (as measured by specific conductance) in San Pablo and Suisun bays, suggesting that the center of distribution for both species was seaward and that individuals were more abundant in the San Pablo and Suisun bays as water was shifted inland on flood and high tides. Similarly, threadfin shad and striped bass had negative associations with salinity in Suisun Bay, suggesting that both species became more abundant in the study area as water shifted seaward on ebb and low tides. This is expected for the oligohaline threadfin shad (Moyle 2002), and juvenile striped bass are known to be abundant in the inland areas of Suisun Bay (Sommer et al. 2011; Zeug et al. 2017; Feyrer et al. 2021). Although we would expect demersal fish and shrimp distribution to respond to broad variation along the estuarine salinity gradient (Buchheister et al. 2013; Feyrer et al. 2015), we did not see strong associations between demersal organism (fish and shrimp) and salinity at the tidal timescales evaluated in this study.

Nekton exhibited weak or nonexistent relationships with turbidity in 2017 (San Pablo Bay), which may have been due to the low turbidities encountered during sampling in 2017; turbidities greater than 15 FNU were only infrequently encountered within 2 m of the substrate and were not encountered higher in the water column. Behavioral responses to turbidity are often associated with a species- or system-specific light threshold (McIninch and Hocutt 1987; Gray et al. 2014), which likely was not reached in our study area. Turbidities in 2018 (Suisun Bay) were higher, and relationships between turbidity and nekton were commensurately stronger. Pelagic fish are typically more efficiently captured by trawl gears in low visibility conditions (Walsh 1991; Peterson and Barajas 2018); however, the lack of clear positive relationships with turbidity by surface-oriented fish suggests that turbidity-driven sampling efficiency may have been insufficient to drive observed fish densities.

In contrast, the density of longfin smelt and striped bass increased at the surface during more turbid conditions, suggesting that turbidity could contribute to vertical movement for these species. Turbidity-mediated vertical migrations have been documented for many species and are typically tied to foraging or predator avoidance (Kaartvedt et al. 2012; Whitton et al. 2020). Because vertical shifts by subadult

longfin smelt and striped bass were associated with elevated turbidity rather than tide, vertical movements in this study area may be related to predator avoidance rather than to maintaining estuarine position, unlike the larvae of each species (Bennett et al. 2002).

The Complexity of Tide

Tides can influence nekton distribution through fluctuations in the salinity field and through physical hydrodynamics and interactions with other environmental conditions (e.g., diel cycles and turbidity). This suggests that the interaction between light intensity and tide direction or amplitude partially drives organism behavior similar to observations in other estuaries (Viehman and Zydlewski 2017). Vertical position differences in San Pablo Bay may have resulted from fishes making vertical movements to follow prey items or take direct advantage of tidal currents to maintain position within the estuary (Forward and Tankersley 2001). These transport mechanisms are frequently used by larval or juvenile fishes (Fortier and Leggett 1983; Bennett et al. 2002) and zooplankton (Kimmerer et al. 1998; Simons et al. 2006). Although vertical position of nekton in San Pablo Bay showed variability across tides, additional data would be needed to isolate clear mechanisms. Vertical migrations have been observed in other San Francisco Estuary studies but can be highly specific. Vertical migrations may only be observed at certain tides (e.g., big ebb at night) and can be dependent on location or season (Bennett et al. 2002), hydrodynamic conditions (Kimmerer et al. 2002), or life history needs (i.e., spawning migrations; Verhelst et al. 2018). Further study that includes depth-specific prey or predator densities and a wider range of turbidities would help to differentiate mechanisms driving vertical migrations by fishes in San Pablo Bay.

Lateral migrations also can facilitate selective tidal-stream transport by a variety of migratory species as an alternate mechanism for holding position and avoiding advection (Forward and Tankersley 2001). For example, the shoal-ward distribution of American shad on ebb and low tide and the channel-ward distribution on flood and high tide observed in this study are consistent with selective tidal stream transport intended to facilitate retention. An affinity for lower-velocity shoal habitats at ebb tide would minimize seaward advection while maximizing inland transport in the channels on flood tides. Similar behavior has been documented for other species in the San Francisco Estuary (Feyrer et al. 2013; Bennett and Burau 2015). Shoal-ward shifts by American shad may also provide some other habitat benefit, such as food availability at lower tides.

Northern anchovy were more abundant at higher salinities, and we observed high catches of northern anchovy from peak flood to high tide. During this period, more individuals were observed in the channel on peak flood tide with the

proportion of individuals on the shoal increasing through high tide. This suggests that northern anchovy may be moving upstream with the flood tide in the channel and then moving to the shoals after entering Suisun Bay. This shoal-ward shift may be to avoid farther inland movement, for the purposes of foraging, or for predator avoidance. The lateral position of *C. franciscorum* was also highly variable across the tide cycle, in contrast with Shokihaze and yellowfin gobies and *Palaemon* species, which exhibited little variability in lateral position.

These movement patterns indicate that both midwater and otter trawls could identify tidal variability in lateral position because tidal variability was observed for certain species and not observed for other species. Logistical constraints prevented samples from being collected from all combinations of habitat and tide phase, but we found strong evidence that tidal phase mediates vertical and lateral distributions for many resident species. Additional data would help to further quantify the underlying mechanisms which drive observed distributional differences across tide phases.

Vertical and lateral migrations made by nekton species in this study are likely to be stronger during spawning and recruitment periods. Selective tidal-stream transport is often used by fishes to conserve energy during spawning migrations, particularly for smaller and poor-swimming fishes (Forward and Tankersley 2001; Silva et al. 2017) and by larval and juvenile fishes to maintain position in beneficial nursery habitats (Holt et al. 1989; Islam et al. 2007). The reproductive period for most species in this study is typically in the spring or early summer; our sampling was conducted in autumn, outside of this reproductive window. In addition, variability in estuarine conditions can elevate the necessity for position-maintaining behavior (Power 1997; Bittler et al. 2014). In the San Francisco Estuary characterized by a Mediterranean climate, river outflow is typically lowest in late-summer and early-autumn seasons (the season of this study). Thus, the intensity of position-maintaining vertical and/or lateral shifts in distribution will likely be higher in spring or early summer, as increased river outflow coincides with spawning migrations or larval recruitment. This context is important given that we documented species-specific distribution patterns associated with specific combinations of diel, tidal, and water quality conditions in autumn, when these patterns may be less pronounced.

Active management of water exports in the San Francisco Estuary results in a relatively constant salinity field except during periods of high spring outflow (Kimmerer et al. 2013). The salinity field is contingent on runoff and varies most once runoff exceeds current water management operations. Thus, although this study was only implemented in one season (autumn), the underlying hydrodynamic processes (i.e., tides) that affect nekton distribution are generally broadly applicable throughout the year. However, the

San Francisco Estuary is hydrodynamically complex, with a series of constrictions and embayments severely constraining tidal water movement and resulting in high spatial heterogeneity. This geomorphic variability suggests that the specifics of our findings may not be applicable everywhere within the San Francisco Estuary. Relationships between nekton, habitat, and tides may change based on the specifics of tidal currents and bathymetry. Because of this complexity, care must be taken when extrapolating to unstudied areas. A focused understanding of vertical and lateral distributions of fishes and other nekton with respect to tide, the range of environmental conditions, and a specific region is warranted.

Management Implications

The potential for estuarine nekton to adjust position on fine spatiotemporal scales (e.g., within a tidal cycle and adjacent shoal/channel habitats) is important for evaluating ecological processes and critical for contextualizing data collected at coarser spatiotemporal scales (e.g., fisheries-independent monitoring surveys). Fisheries-independent monitoring surveys often sample at fixed time intervals and/or at fixed sampling stations at spatiotemporal scales designed to detect long-term abundance trends in economically important or at-risk species. However, these surveys often do not take diel migrations, tide, or other physical processes into account and can therefore have substantial unmeasured observational bias limiting fine-scale or process-based inference (e.g., tidal aliasing; Bennett and Burau 2015; Zhao et al. 2017). For example, despite low catches, we observed higher densities of longfin smelt at the bottom of the water column and on the shoal with evidence for light-mediated surface-ward movement. These relationships could have significant implications for interpreting monitoring data because declining suspended sediment has contributed to estuary-wide turbidity declines (Wright and Schoellhamer 2004; Hestir et al. 2013), which may complicate trawl-based survey design for monitoring species such as longfin smelt and striped bass (Peterson and Barajas 2018). Studies such as this can provide context to interpret long-term monitoring results in a way that may ultimately aid in process-based inference and management.

Data collected at a higher spatiotemporal resolution could help identify mechanisms driving vertical and lateral migrations by nekton, including longfin smelt. Specifically, it is unclear to what extent observed relationships represent estuary-wide habitat associations or behavioral responses to unmeasured habitat variables that are unique to San Pablo and Suisun bays. For example, the observed shoal-centric distribution of longfin smelt is inconsistent with data from channel and shoal monitoring stations (Rosenfield and Baxter 2007), which observed higher longfin smelt densities in channel stations. This discrepancy in longfin smelt distribution could indicate something unique to our sampling locations, a change in habitat

association through time, a gap in monitoring data collection, or limitations of our dataset. For example, the highly constrained Carquinez Strait (Fig. 1) has notably fast water velocities for the San Francisco Estuary (Monismith et al. 1996), and nearby shoal-ward shifts by American shad and northern anchovy at certain tides may not be as pronounced in lower velocity regions. Catches of longfin smelt in this study were low, but further efforts to refine our understanding of their fine-scale habitat distribution may be complicated by the severity of longfin smelt decline in the San Francisco Estuary (Sommer et al. 2007; Hobbs et al. 2017), thus illustrating the importance of proactively evaluating organism-habitat relationships while the population is abundant enough to provide inference. Understanding the complex interactions between nekton behavior, habitat type and availability, and environmental conditions at multiple spatial and temporal scales is necessary to assess the wide range of strategies driving microhabitat usage in estuaries. This improved understanding could lead to improvements in nekton monitoring and generally support ecological-based management.

Supplementary Information The online version contains supplementary material available at <https://doi.org/10.1007/s12237-024-01351-w>.

Acknowledgements Numerous individuals, including E. Clark, J. Clause, M.J. Farruggia, E. Gusto, J. Kathan, V. Violette, O. Patton, and T. Violette assisted with field work. We thank Brock Huntsman for conversation and statistical advice and Paul Stumpner and the two anonymous reviewers for providing comments that greatly improved this manuscript. Any use of trade, firm, or product names is for descriptive purposes only and does not imply endorsement by the U.S. Government.

Funding This study was funded by the State Water Contractors, Metropolitan Water District, and the California Department of Fish and Wildlife.

Data Availability Original data collected in support of this study (nekton sampling and discrete water quality measurements) can be accessed from Steinke et al. (2019; <https://doi.org/https://doi.org/10.5066/F7SF2VF5>). Tide stage data were obtained from the National Oceanic and Atmospheric Administration's Tides and Currents Program (National Oceanographic and Atmospheric Administration 2023). Tide stage in meters relative to mean lower low water was obtained for San Pablo Bay from Richmond (site 9,414,863; latitude 37.9234; longitude - 122.4089) and for Suisun Bay from Martinez-Amorco Pier (site 9,415,102; latitude 38.0346; longitude - 122.1252).

Open Access This article is licensed under a Creative Commons Attribution 4.0 International License, which permits use, sharing, adaptation, distribution and reproduction in any medium or format, as long as you give appropriate credit to the original author(s) and the source, provide a link to the Creative Commons licence, and indicate if changes were made. The images or other third party material in this article are included in the article's Creative Commons licence, unless indicated otherwise in a credit line to the material. If material is not included in the article's Creative Commons licence and your intended use is not permitted by statutory regulation or exceeds the permitted use, you will need to obtain permission directly from the copyright holder. To view a copy of this licence, visit <http://creativecommons.org/licenses/by/4.0/>.

References

- Amorim, E., S. Ramos, M. Elliott, and A.A. Bordalo. 2018. Dynamic habitat use of an estuarine nursery seascape: ontogenetic shifts in habitat suitability of the European flounder (*Platichthys flesus*). *Journal of Experimental Marine Biology and Ecology* 506: 49–60. <https://doi.org/10.1016/j.jembe.2018.05.011>.
- Barros, A., J.A. Hobbs, M. Willmes, C.M. Parker, M. Bisson, N.A. Fanguie, A.L. Rypel, and L.S. Lewis. 2022. Spatial heterogeneity in prey availability, feeding success, and dietary selectivity for the threatened longfin smelt. *Estuaries and Coasts*. Springer: 1–14. <https://doi.org/10.1007/s12237-021-01024-y>.
- Bennett, W.A., and J.R. Burau. 2015. Riders on the storm: selective tidal movements facilitate the spawning migration of threatened delta smelt in the San Francisco Estuary. *Estuaries and Coasts* 38: 826–835. <https://doi.org/10.1007/s12237-014-9877-3>.
- Bennett, W.A., W.J. Kimmerer, and J.R. Burau. 2002. Plasticity in vertical migration by native and exotic estuarine fishes in a dynamic low-salinity zone. *Limnology and Oceanography* 47: 1496–1507. <https://doi.org/10.4319/lo.2002.47.5.1496>.
- Berglund, A. 1982. Coexistence, size overlap and population regulation in tidal vs. non-tidal Palaemon prawns. *Oecologia* 54: 1–7. <https://doi.org/10.1007/BF00541099>.
- Bever, A.J., M.L. MacWilliams, B. Herbold, L.R. Brown, and F.V. Feyrer. 2016. Linking hydrodynamic complexity to delta smelt (*Hypomesus transpacificus*) distribution in the San Francisco estuary, USA. *San Francisco Estuary and Watershed Science* 14. <https://doi.org/10.15447/sfews.2016v14iss1art3>.
- Bittler, K.M., L.P. Scheef, and E.J. Buskey. 2014. Freshwater inflows and blue crabs: The influence of salinity on selective tidal stream transport. *Marine Ecology Progress Series* 514: 137–148. <https://doi.org/10.3354/meps10990>.
- Bollens, S.M., and B.W. Frost. 1989. Zooplanktivorous fish and variable diel vertical migration in the marine planktonic copepod *Calanus pacificus*. *Limnology and Oceanography* 34: 1072–1083. <https://doi.org/10.4319/lo.1989.34.6.1072>.
- Bottom, D.L., and K.K. Jones. 1990. Species composition, distribution, and invertebrate prey of fish assemblages in the Columbia River estuary. *Progress in Oceanography* 25: 243–270. [https://doi.org/10.1016/0079-6611\(90\)90009-Q](https://doi.org/10.1016/0079-6611(90)90009-Q).
- Brown, T., and K.A. Hieb. 2014. Status of the Siberian prawn, *Exopalaemon modestus*, in the San Francisco Estuary. *San Francisco Estuary and Watershed Science* 12. <https://doi.org/10.15447/sfews.2014v12iss1art4>.
- Buchheister, A., C.F. Bonzek, J. Gartland, and R.J. Latour. 2013. Patterns and drivers of the demersal fish community of Chesapeake Bay. *Marine Ecology Progress Series* 481: 161–180. <https://doi.org/10.3354/meps10253>.
- Bürkner, P.-C. 2017. brms: an R package for Bayesian multilevel models using stan. *Journal of Statistical Software* 80: 1–28. <https://doi.org/10.18637/jss.v080.i01>.
- California Fish and Game Commission. Notice of findings: longfin smelt (*Spirinchus thaleichthys*). 2009. Woodland, CA.
- Chigbu, P., T.H. Sibley, and D.A. Beauchamp. 1998. Abundance and distribution of *Neomysis mercedis* and a major predator, longfin smelt (*Spirinchus thaleichthys*) in Lake Washington. *Hydrobiologia* 386: 167–182. <https://doi.org/10.1023/A:1003537122340>.
- Cloern, J.E., and A.D. Jassby. 2012. Drivers of change in estuarine-coastal ecosystems: discoveries from four decades of study in San Francisco Bay. *Reviews of Geophysics*. <https://doi.org/10.1029/2012RG000397>.
- Cohen, A.N., and J.T. Carlton. 1998. Accelerating invasion rate in a highly invaded estuary. *Science* 279: 555–558. <https://doi.org/10.1126/science.279.5350.555>.
- Colombano, D.D., J.M. Donovan, D.E. Ayers, T.A. O’Rear, and P.B. Moyle. 2020. Tidal effects on marsh habitat use by three fishes in the San Francisco Estuary. *Environmental Biology of Fishes* 103: 605–623. <https://doi.org/10.1007/s10641-020-00973-w>.
- Dornburg, A., E.J. Forrester, J.A. Moore, T.L. Iglesias, A. Jones, L. Rao, and D.L. Warren. 2017. An assessment of sampling biases across studies of diel activity patterns in marine ray-finned fishes (Actinopterygii). *Bulletin of Marine Science* 93: 611–639. <https://doi.org/10.5343/bms.2016.1016>.
- Feyrer, F., J.E. Cloern, L.R. Brown, M.A. Fish, K.A. Hieb, and R.D. Baxter. 2015. Estuarine fish communities respond to climate variability over both river and ocean basins. *Global Change Biology* 21: 3608–3619. <https://doi.org/10.1111/gcb.12969>.
- Feyrer, F., D. Portz, D. Odum, K. B. Newman, T. Sommer, D. Contreras, R. Baxter, S. B. Slater, D. Sereno, and E. Van Nieuwenhuysse. 2013. SmeltCam: underwater video codend for trawled nets with an application to the distribution of the imperiled delta smelt. *PLoS One* 8. Public Library of Science San Francisco, USA: e67829. <https://doi.org/10.1371/journal.pone.0067829>.
- Feyrer, F., M.J. Young, B.M. Huntsman, and L.R. Brown. 2021. Distinguishing stationary and dynamic estuarine fish habitat to inform conservation: species-specific responses to physical habitat and water quality in San Francisco Estuary. *Marine and Coastal Fisheries* 13: 559–574. <https://doi.org/10.1002/mcf2.10183>.
- Fortier, L., and W. Leggett. 1983. Vertical migrations and transport of larval fish in a partially mixed estuary. *Canadian Journal of Fisheries and Aquatic Sciences* 40: 1543–1555. <https://doi.org/10.1139/f83-179>.
- Forward, R. B., and R. A. Tankersley. 2001. Selective tidal-stream transport of marine animals. In *Oceanography and Marine Biology, an Annual Review*, 39:305–353. London: CRC Press.
- Fregoso, T.A., R.-F. Wang, E. Ateljevich, and B.E. Jaffe. 2017. *A new seamless, high-resolution digital elevation model of the San Francisco Bay-Delta Estuary, California*. US Geological Survey.
- González-Ortegón, E., J.A. Cuesta, E. Pascual, and P. Drake. 2010. Assessment of the interaction between the white shrimp, *Palaemon longirostris*, and the exotic oriental shrimp, *Palaemon macrodactylus*, in a European estuary (SW Spain). *Biological Invasions* 12: 1731–1745. <https://doi.org/10.1007/s10530-009-9585-2>.
- Gray, S.M., F.M.E. Bieber, and Laura H. McDonnell, Lauren J. Chapman, and N. E. Mandrak. 2014. Experimental evidence for species-specific response to turbidity in imperilled fishes. *Aquatic Conservation: Marine and Freshwater Ecosystems* 24: 546–560. <https://doi.org/10.1002/aqc.2436>.
- Greenwood, M.F. 2007. Nekton community change along estuarine salinity gradients: can salinity zones be defined? *Estuaries and Coasts* 30: 537–542. <https://doi.org/10.1007/BF03036519>.
- Grimaldo, L., F. Feyrer, J. Burns, and D. Maniscalco. 2017. Sampling uncharted waters: Examining rearing habitat of larval longfin smelt (*Spirinchus thaleichthys*) in the upper San Francisco Estuary. *Estuaries and Coasts* 40: 1771–1784. <https://doi.org/10.1007/s12237-017-0255-9>.
- Hatfield, S.E. 1985. Seasonal and interannual variation in distribution and population abundance of the shrimp *Crangon franciscorum* in San Francisco Bay. In *Temporal dynamics of an estuary: San Francisco Bay*, 30:199–210. Developments in Hydrobiology. Dordrecht: Springer.
- Hestir, E.L., D.H. Schoellhamer, T. Morgan-King, and S.L. Ustin. 2013. A step decrease in sediment concentration in a highly modified tidal river delta following the 1983 El Niño floods. *Marine Geology* 345: 304–313. <https://doi.org/10.1016/j.margeo.2013.05.008>.
- Hobbs, J., P.B. Moyle, N. Fanguie, and R.E. Connon. 2017. Is extinction inevitable for delta smelt and longfin smelt? An opinion and

- recommendations for recovery. *San Francisco Estuary and Watershed Science* 15. <https://doi.org/10.15447/sfews.2017v15iss2art2>.
- Holt, S.A., G.J. Holt, and C.R. Arnold. 1989. Tidal stream transport of larval fishes into non-stratified estuaries. *Rapp PV Reun Cons Int Explor Mer* 191: 100–104.
- Huntsman, B.M., B. Mahardja, and S.M. Bashevkin. 2022. Relative bias in catch among long-term fish monitoring surveys within the San Francisco Estuary. *San Francisco Estuary and Watershed Science* 20. <https://doi.org/10.15447/sfews.2022v20iss1art3>.
- Islam, M., M. Hibino, M. Tanaka, et al. 2007. Tidal and diurnal variations in larval fish abundance in an estuarine inlet in Ariake Bay, Japan: implication for selective tidal stream transport. *Ecological Research* 22: 165–171. <https://doi.org/10.1007/s11284-006-0001-4>.
- Kaartvedt, S., T.A. Klevjer, and D.L. Aksnes. 2012. Internal wave-mediated shading causes frequent vertical migrations in fishes. *Marine Ecology Progress Series* 452: 1–10. <https://doi.org/10.3354/meps09688>.
- Kimmerer, W., J.R. Burau, and W. Bennett. 2002. Persistence of tidally-oriented vertical migration by zooplankton in a temperate estuary. *Estuaries* 25: 359–371. <https://doi.org/10.1007/BF02695979>.
- Kimmerer, William J., J. Burau, and W. Bennett. 1998. Tidally oriented vertical migration and position maintenance of zooplankton in a temperate estuary. *Limnology and Oceanography* 43: 1697–1709. <https://doi.org/10.4319/lo.1998.43.7.1697>.
- Kimmerer, Wim J. 2006. Response of anchovies dampens effects of the invasive bivalve *Corbula amurensis* on the San Francisco Estuary foodweb. *Marine Ecology Progress Series* 324: 207–218. <https://doi.org/10.3354/meps324207>.
- Kimmerer, Wim J., M.L. MacWilliams, and E.S. Gross. 2013. Variation of fish habitat and extent of the low-salinity zone with freshwater flow in the San Francisco Estuary. *San Francisco Estuary and Watershed Science* 11. <https://doi.org/10.15447/sfews.2013v11iss4art1>.
- Koslow, J.A. 1981. Feeding selectivity of schools of northern anchovy, *Engraulis mordax*, in the Southern California Bight. *Fishery Bulletin* 79: 131–142.
- Kuprijanov, I., K. Herkül, and J. Kotta. 2017. Ecological niche differentiation between native and non-native shrimps in the northern Baltic Sea. *Aquatic Ecology* 51: 389–404. <https://doi.org/10.1007/s10452-017-9624-5>.
- Lewis, L.S., M. Willmes, A. Barros, P.K. Crain, and J.A. Hobbs. 2020. Newly discovered spawning and recruitment of threatened longfin smelt in restored and underexplored tidal wetlands. *The Scientific Naturalist*. <https://doi.org/10.1002/ecy.2868>.
- Mac Nally, R., J.R. Thomson, W.J. Kimmerer, F. Feyrer, K.B. Newman, A. Sih, W.A. Bennett, et al. 2010. Analysis of pelagic species decline in the upper San Francisco Estuary using multivariate autoregressive modeling (MAR). *Ecological Applications* 20: 1417–1430. <https://doi.org/10.1890/09-1724.1>.
- Mahardja, B., M. Young, B. Schreier, and T. Sommer. 2017. Understanding imperfect detection in a San Francisco Estuary long-term larval and juvenile fish monitoring programme. *Fisheries Management and Ecology* 24: 488–503. <https://doi.org/10.1111/fme.12257>.
- McIninch, S., and C. Hocutt. 1987. Effects of turbidity on estuarine fish response to strobe lights. *Journal of Applied Ichthyology* 3: 97–105. <https://doi.org/10.1111/j.1439-0426.1987.tb00460.x>.
- Mehner, T. 2012. Diel vertical migration of freshwater fishes – proximate triggers, ultimate causes and research perspectives. *Freshwater Biology* 57: 1342–1359. <https://doi.org/10.1111/j.1365-2427.2012.02811.x>.
- Merz, J.E., P.S. Bergman, J.F. Melgo, and S. Hamilton. 2013. Longfin smelt: Spatial dynamics and ontogeny in the San Francisco Estuary, California. *California Fish and Game* 99: 122–148.
- Mitchell, L., and R. Baxter. 2021. Examining retention-at-length of pelagic fishes caught in the fall midwater trawl survey. *San Francisco Estuary and Watershed Science*. <https://doi.org/10.15447/sfews.2021v19iss2art5>.
- Mitchell, L., K. Newman, and R. Baxter. 2017. A covered cod-end and tow-path evaluation of midwater trawl gear efficiency for catching delta smelt (*Hypomesus transpacificus*). *San Francisco Estuary and Watershed Science*. <https://doi.org/10.15447/sfews.2017v15iss4art3>.
- Monismith, S. G., J. R. Burau, and M. Stacey. 1996. Stratification dynamics and gravitational circulation in northern San Francisco Bay. *San Francisco Bay: The Ecosystem* 123. Citeseer: 153.
- Moyle, P.B. 2002. *Inland fishes of California: Revised and expanded*. Berkeley, CA: University of California Press.
- National Oceanographic and Atmospheric Administration. 2023. Tides and Currents. <https://tidesandcurrents.noaa.gov/>. Accessed January 25.
- Neilson, J., and R. Perry. 1990. *Diel vertical migrations of marine fishes: An obligate or facultative process? In Advances in Marine Biology*, 26: 115–168. Elsevier.
- Paterson, A., and A. Whitfield. 2000. Do shallow-water habitats function as refugia for juvenile fishes? *Estuarine, Coastal and Shelf Science* 51: 359–364. <https://doi.org/10.1006/ecss.2000.0640>.
- Peterson, J. T., and M. F. Barajas. 2018. An evaluation of three fish surveys in the San Francisco Estuary, 1995–2015. *San Francisco Estuary and Watershed Science* 16.
- Peterson, M.S. 2003. A conceptual view of environment-habitat-production linkages in tidal river estuaries. *Reviews in Fisheries Science* 11: 291–313. <https://doi.org/10.1080/10641260390255844>.
- Power, J.H. 1997. Time and tide wait for no animal: seasonal and regional opportunities for tidal stream transport or retention. *Estuaries* 20: 312–318. <https://doi.org/10.2307/1352346>.
- Quinn, T.P., C.J. Sergeant, A.H. Beaudreau, and D.A. Beauchamp. 2012. Spatial and temporal patterns of vertical distribution for three planktivorous fishes in Lake Washington. *Ecology of Freshwater Fish* 21: 337–348. <https://doi.org/10.1111/j.1600-0633.2012.00554.x>.
- R Core Team. 2022. R: a language and environment for statistical computing. Vienna, Austria: R Foundation for Statistical Computing.
- Rosenfield, J.A., and R.D. Baxter. 2007. Population dynamics and distribution patterns of longfin smelt in the San Francisco Estuary. *Transactions of the American Fisheries Society* 136: 1577–1592. <https://doi.org/10.1577/T06-148.1>.
- Rountree, R.A., and K.W. Able. 2007. Spatial and temporal habitat use patterns for salt marsh nekton: implications for ecological functions. *Aquatic Ecology* 41: 25–45. <https://doi.org/10.1007/s10452-006-9052-4>.
- Scheuerell, M.D., and D.E. Schindler. 2003. Diel vertical migration by juvenile sockeye salmon: empirical evidence for the antipredation window. *Ecology* 84: 1713–1720. [https://doi.org/10.1890/0012-9658\(2003\)084\[1713:DVMBJS\]2.0.CO;2](https://doi.org/10.1890/0012-9658(2003)084[1713:DVMBJS]2.0.CO;2).
- Schoellhamer, D.H. 2000. Influence of salinity, bottom topography, and tides on locations of estuarine turbidity maxima in northern San Francisco Bay. *In Proceedings in Marine Science* 3: 343–357 Elsevier.
- Siegfried, C.A. 1980. Seasonal abundance and distribution of Crangon franciscorum and Palaemon macrodactylus (Decapoda, Caridea) in the San Francisco Bay-Delta. *The Biological Bulletin* 159: 177–192. <https://doi.org/10.2307/1541017>.
- Silva, S., C. Macaya-Solis, and M.C. Lucas. 2017. Energetically efficient behaviour may be common in biology, but it is not universal: A test of selective tidal stream transport in a poor swimmer. *Marine Ecology Progress Series* 584: 161–174. <https://doi.org/10.3354/meps12352>.
- Simons, R.D., S.G. Monismith, L.E. Johnson, G. Winkler, and F.J. Saucier. 2006. Zooplankton retention in the estuarine transition zone of the St.

- Lawrence Estuary. *Limnology and Oceanography* 51: 2621–2631. <https://doi.org/10.4319/lo.2006.51.6.2621>.
- Sommer, T., C. Armor, R. Baxter, R. Breuer, L. Brown, M. Chotkowski, S. Culberson, et al. 2007. The collapse of pelagic fishes in the upper San Francisco Estuary. El colapso de los peces pelagicos en la cabecera del Estuario San Francisco. *Fisheries* 32: 270–277. [https://doi.org/10.1577/1548-8446\(2007\)32\[270:TCOPFI\]2.0.CO;2](https://doi.org/10.1577/1548-8446(2007)32[270:TCOPFI]2.0.CO;2).
- Sommer, T., F. Mejia, K. Hieb, R. Baxter, E. Loboschefskey, and F. Loge. 2011. Long-term shifts in the lateral distribution of age-0 striped bass in the San Francisco Estuary. *Transactions of the American Fisheries Society* 140: 1451–1459. <https://doi.org/10.1080/00028487.2011.630280>.
- Steinke, D.A., M.J. Young, and F.V. Feyrer. 2019. Vertical distribution of longfin smelt in the San Francisco Estuary (ver. 2.0, August 2019). U. S. Geological Survey.
- Stompe, D.K., P.B. Moyle, A. Kruger, and J.R. Durand. 2020. Comparing and integrating fish surveys in the San Francisco Estuary: why diverse long-term monitoring programs are important. *San Francisco Estuary and Watershed Science* 18. <https://doi.org/10.15447/sfews.2020v18iss2art4>.
- Tempel, T.L., T.D. Malinich, J. Burns, A. Barros, C.E. Burdi, and J.A. Hobbs. 2021. The value of long-term monitoring of the San Francisco Estuary for delta smelt and longfin smelt. *California Fish and Game* 107. California Fish and Game Editor 1416 Ninth St, Sacramento, CA 95814 USA: 148–171. <https://doi.org/10.51492/cfwj.cesasi.7>.
- Thayer, G.W., and A.J. Chester. 1989. Distribution and abundance of fishes among basin and channel habitats in Florida Bay. *Bulletin of Marine Science* 44: 200–219.
- Thomson, J.R., W.J. Kimmerer, L.R. Brown, K.B. Newman, R.M. Nally, W.A. Bennett, F. Feyrer, and E. Fleishman. 2010. Bayesian change point analysis of abundance trends for pelagic fishes in the upper San Francisco Estuary. *Ecological Applications* 20: 1431–1448. <https://doi.org/10.1890/09-0998.1>.
- U.S. Fish and Wildlife Service. 2023. Endangered species status for the San Francisco Bay-delta distinct population segment of the longfin smelt. Docket No. FWS–R8–ES–2022–0082. Washington, D.C.: U.S. Fish and Wildlife Service.
- Vehtari, A., J. Gabry, M. Magnusson, Y. Yao, P.-C. Bürkner, T. Paananen, and A. Gelman. 2022. loo: efficient leave-one-out cross-validation and WAIC for Bayesian models.
- Verhelst, P., S. Bruneel, J. Reubens, J. Coeck, P. Goethals, D. Oldoni, T. Moens, and A. Mouton. 2018. Selective tidal stream transport in silver European eel (*Anguilla anguilla* L.) – migration behaviour in a dynamic estuary. *Estuarine, Coastal and Shelf Science* 213: 260–268. <https://doi.org/10.1016/j.ecss.2018.08.025>.
- Viehman, H.A., and G.B. Zydlewski. 2017. Multi-scale temporal patterns in fish presence in a high-velocity tidal channel. *PLoS One* 12. Public Library of Science San Francisco, CA USA: e0176405. <https://doi.org/10.1371/journal.pone.0176405>.
- Walsh, S. 1991. Diel variation in availability and vulnerability of fish to a survey trawl. *Journal of Applied Ichthyology* 7: 147–159. <https://doi.org/10.1111/j.1439-0426.1991.tb00521.x>.
- Whitton, T.A., S.E. Jackson, J.G. Hiddink, B. Scouling, D. Bowers, B. Powell, T. D'Urban Jackson, L. Gimenez, and A.G. Davies. 2020. Vertical migrations of fish schools determine overlap with a mobile tidal stream marine renewable energy device. *Journal of Applied Ecology* 57: 729–741. <https://doi.org/10.1111/1365-2664.13582>.
- Wright, S.A., and D.H. Schoellhamer. 2004. Trends in the sediment yield of the Sacramento River, California, 1957–2001. *San Francisco Estuary and Watershed Science* 2. <https://doi.org/10.15447/sfews.2004v2iss2art2>.
- Yao, Y., A. Vehtari, D. Simpson, and A. Gelman. 2017. Using stacking to average Bayesian predictive distributions. *Bayesian Analysis*. <https://doi.org/10.1214/17-BA1091>.
- Young, M.J., K.A. Berridge, T. O'Rear, P.B. Moyle, and J.R. Durand. 2017. Habitat partitioning by native and alien fishes and decapods in novel habitats of the upper San Francisco Estuary. *Biological Invasions* 19: 2693–2710. <https://doi.org/10.1007/s10530-017-1477-2>.
- Zeug, S.C., F.V. Feyrer, A. Brodsky, and J. Melgo. 2017. Piscivore diet response to a collapse in pelagic prey populations. *Environmental Biology of Fishes* 100: 947–958. <https://doi.org/10.1007/s10641-017-0618-x>.
- Zhao, J., J. Cao, S. Tian, Y. Chen, S. Zhang, and X. Zhou. 2017. Influence of sampling frequency on detectability of fish community and fish species in a fishery-independent survey. *Aquaculture and Fisheries* 2: 94–102. <https://doi.org/10.1016/j.aaf.2017.03.003>.